Colloid Polym Sci 279:1112–1117 (2001)

ORIGINAL CONTRIBUTION

P. Calandra
A. Longo
V. Turco Liveri

Preparation and characterisation of Na_2S and $ZnSO_4$ nanoparticles in water/sodium bis(2-ethylhexyl)sulphosuccinate/*n*-heptane microemulsions

Received: 09 February 2001
Accepted: 19 March 2001

P. Calandra · V. Turco Liveri (✉)
Department of Physical Chemistry
University of Palermo
Viale delle Scienze Parco D'Orleans II
90128 Palermo, Italy
e-mail: turco@unipa.it

A. Longo
ICTPN, Istituto di Chimica e
Tecnologia dei Prodotti naturali
Via U. La Malfa 153
90146 Palermo
Italy

Abstract The preparation procedure for nanoparticles of the water-soluble salts Na_2S and $ZnSO_4$, two commonly used reagents to synthesise ZnS nanoparticles, by evaporation of volatile components of salt-containing water-in-oil microemulsions is described. In suitable conditions, the evaporation leads to the formation of dry salt–surfactant composites and to the formation of Na_2S or $ZnSO_4$ nanoparticles. It was found that the salt–surfactant composites can be totally redissolved in a dry apolar organic solvent allowing the formation of virtually water-free solutions containing a considerable amount of the water-soluble salts. The presence of nanoparticles in these solutions and in the composites has been proved by small-angle X-ray scattering and transmission electron microscopy, respectively. By mixing these solutions, the solid–solid reaction between Na_2S and $ZnSO_4$ nanoparticles leading to the formation of very small-sized ZnS nanoparticles has been ascertained by UV spectrophotometry.

Key words Water-soluble inorganic salts · Nanoparticles · Nanoparticle–nanoparticle reaction · Water-in-oil microemulsions

Introduction

Recently, interest in the synthesis and physicochemical characterisation of nanosized particles (diameter 1–100 nm) has been increasing steadily. There are several reasons for this interest. First of all, owing to the great value of the surface-to-volume ratio, applications of these materials can be found in processes such as chemical or photochemical catalysis and enhanced physical or chemical adsorption. Moreover, the electronic structure of a nanoparticle is in some cases very different from that of bulk material and an isolated atom/molecule, leading to exotic physicochemical properties which cannot be found in conventional materials [1, 2]. From a different prospect, the synthesis of nanoparticles is the necessary step to realise highest density data storage devices, nanosensors, nanocarriers and nanomachines [3].

Given the importance of nanoparticles in modern technology, in the last few decades much effort has been directed to set up efficient protocols for their synthesis. In particular, since nanoparticles tend to grow spontaneously and their properties are critically size-dependent, a useful technique of synthesis should allow fine size control and nanoparticle passivation [4–6]. In order to achieve these goals, the use of water-in-oil (w/o) microemulsions as a solvent and reaction media has been suggested because they offer not only an alternative route to other synthetic methods but also specific advantages [7, 8].

These advantages are mainly a consequence of the peculiar structural and dynamic properties of such systems. In fact, from a microscopic point of view, w/o microemulsions are constituted by water nanodroplets coated by a monolayer of opportunely oriented surfactant molecules (reversed micelles) dispersed in an apolar

solvent. Their size is mainly controlled by the water-to-surfactant molar ratio (R_w). Water-containing reversed micelles are thus confined aqueous nanoregions, which can be thought of as nanoreactors, so, if two microemulsions containing appropriate reagents are mixed, the intermicellar material exchange process allows the reagents to come into contact and to react to form nanoparticles constrained to reside inside the micellar cores. The size of the nanoreactors, their dispersion in the apolar medium and the nature of surfactant head group could allow the stabilisation of size-controlled nanoparticles, thus preventing them from unlimited growth [9, 10]. Obviously, using this technique, only the synthesis of nanoparticles of water-insoluble substances can be achieved [11–14].

Recently, however, a new procedure for the preparation of nanoparticles of water-soluble salts by means of w/o microemulsions has been considered: it is based on the complete evaporation of volatile components (water and apolar solvent) of a salt-containing w/o microemulsion, followed by resuspension of the salt/surfactant composite in the apolar solvent. Under suitable conditions, the progressive elimination of water from the micelles owing to the evaporation process and the continuous intermicellar exchange of materials, leads to the accumulation of the salt inside the micellar core forming nanoparticles coated by a surfactant monolayer. As a consequence of this sort of ''confined crystallisation'', the nanoparticle size and size distribution result from a delicate balance between the nanoparticle tendency to grow without limits and the freezing of their diffusive motion owing to the evaporation of organic solvent. In fact, above a threshold value of the surfactant concentration, the progressive subtraction of the organic solvent leads to a dramatic increase in the system viscosity [15]. Moreover it can be expected that adsorption of surfactant molecules on the nanoparticle surface plays a pivotal role in controlling the nanoparticle size and in stabilising their resuspensions [8, 16].

The aim of this preliminary contribution is to describe the experimental conditions leading to the preparation of stable nanoparticles of the water-soluble salts Na_2S and $ZnSO_4$ using water/sodium bis(2-ethylhexyl)sulphosuccinate (AOT)/*n*-heptane microemulsions. These salts were selected not only to enlarge our knowledge of the preparation of nanoparticles of water-soluble salts but also in view of a novel method to form ZnS nanoparticles based on a solid–solid reaction in a confined space. Semiconductor nanoparticles are in fact very interesting materials because, owing to quantum size effects, they possess size-dependent photophysical and photochemical properties. In particular, the interest in ZnS is justified by its actual or potential importance as a phosphor, in thin-film electroluminescent devices, solar cells, IR windows and photochemical production of hydrogen [17, 18].

Experimental

Materials

AOT (Sigma 98%) was stored in a desiccator and used after at least 1 week. In the dried surfactant, a residual content of 0.2 water molecules for every AOT molecule was found by Fourier transform IR spectroscopy [19]. *n*-Heptane (Aldrich 99%, spectrophotometric grade), zinc sulphate monohydrate (Carlo Erba 98%, Analyticals) and sodium sulphide nonahydrate (Sigma above 98%, ACS reagent) were used as received. Bidistilled water was used in all experiments.

Methods

All samples were prepared by weight. Water/AOT/*n*-heptane w/o microemulsions at various water-to-AOT molar ratios (R_w) were prepared by adding a 0.15 molkg^{-1} AOT/*n*-heptane solution to the appropriate amount of water.

Each salt-containing w/o microemulsion at a given salt-to-AOT molar ratio (R_s), was prepared by adding the appropriate amount of w/o microemulsion to a weighed quantity of salt. Solubilisation of the salt in w/o microemulsions was sped up by ultrasonication. Na_2S-containing w/o microemulsions were used immediately after their preparation because preliminary experiments showed that such microemulsions are not stable over a long time probably owing to the basic hydrolysis of the sulphide ions with formation of volatile H_2S. In contrast, $ZnSO_4$-containing w/o microemulsions showed no ageing effects. At each R_w value, the solubility of Na_2S and $ZnSO_4$ in the w/o microemulsions was determined by visual inspection of samples prepared at various R_s values and kept at constant temperature (25 °C).

The preparation of the salt–surfactant composites was carried out by keeping the salt-containing w/o microemulsions in a desiccator connected to a diaphragm vacuum pump (MZ2C, Vacuubrand). In order to keep the evaporation time constant, the same experimental conditions were used for each sample, i.e. the amount of sample (10 g), the shape and volume of the sample container (50 cm^3 bottle) and the temperature (25 °C). Even if complete evaporation of the volatile components takes about 1 h, all the salt-surfactant composites were kept under vacuum for 1 day. Finally, the salt–surfactant composites were resuspended in the appropriate amount of pure *n*-heptane to give the original AOT concentration.

The small-angle X-ray scattering (SAXS) patterns were recorded using laboratory instrumentation consisting of a Philips PW 1830 X-ray generator providing Cu Kα, Ni filtered (1.5418 Å) radiation with a Kratky small-angle camera in the ''finite-slit-height'' geometry equipped with step scanning motor and scintillation counter. The cell plus solvent contribution was subtracted from each scattering spectrum. Best-fit analyses were performed using the CERN minimisation program called MINUITS.

Transmission electron microscopy (TEM) images were collected using a JEOL 1220 T transmission electron microscope operating at 120 kV representing a suitable acceleration voltage to obtain a good resolution with little radiation damage of the material. The samples for electron microscopy were prepared by placing a drop of the resuspended material onto a carbon–copper grid and allowing the evaporation of the solvent at room temperature.

UV spectra were recorded in the wavelength range 200–400 nm with a PerkinElmer (Lambda-900) spectrophotometer.

Results and discussion

The solubility of Na_2S and $ZnSO_4$ in water/AOT/*n*-heptane microemulsions, expressed as the maximum

salt-to-AOT molar ratio ($R_{s,max}$), is reported as a function of R_w ($R_w = [H_2O]/[AOT]$) in Fig. 1. The observed trends can be rationalised in terms of two opposing factors: the solubilising action of water, predominant at low R_w, leading to an increase in $R_{s,max}$ with increasing R_w and the salt effect on the water solubility in microemulsions, predominant at high R_w, which tends to depress the water solubility and consequently $R_{s,max}$. In fact, at low R_w, the excess salt separates as a solid powder, whereas, at high R_w, it separates as a salt-rich aqueous solution.

After evaporation of the volatile components (water and *n*-heptane) of salt-containing w/o microemulsions, it was observed that the dried salt–AOT composites can be fully dispersed in *n*-heptane giving clear solutions, with the exception of the composites obtained by the evaporation of the salt-containing microemulsions at $R_w = 10$. In this case, full dispersion can be achieved only if $R_s \leq 0.15$. It is worth noting that even if water is virtually absent in the resuspended composites the R_s values of these solutions are higher than the $R_{s,max}$ value obtained at $R_w = 0.2$. Moreover, this procedure allows a considerable amount of salt to be dispersed in an apolar medium. These findings can be explained by postulating that in the resuspended composites the salt is dispersed in the organic solvent as nanoparticles stabilised by a monolayer of oriented surfactant molecules adsorbed at the surface of the nanoparticles. This hypothesis was confirmed by SAXS and TEM.

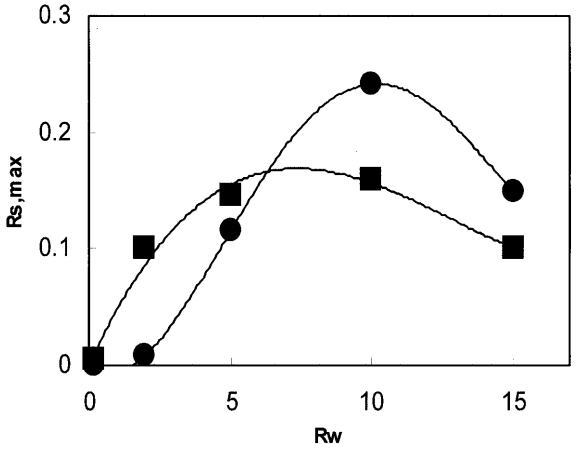

Fig. 1 The $ZnSO_4$ and Na_2S solubilities in water/sodium bis(2-ethylhexyl)sulphosuccinate (*AOT*)/*n*-heptane microemulsions as a function of the water-to-AOT molar ratio (Na_2S: ■, $ZnSO_4$: ●)

Typical X-ray scattering profiles are shown in Fig. 2. A quantitative analysis allowed us to establish that all the SAXS data can be adequately described by a model of noninteracting polydisperse homogenous scattering spheres. In particular the smeared spectra $I(q)$ were fitted with the equation

$$I(q) \propto \int_0^\infty P(t) \int_0^\infty n(r) F^2(x) r^6 \mathrm{d}r\mathrm{d}t \quad . \tag{1}$$

where q is the elastic scattering vector, which has a magnitude of $(4\pi/\lambda)\sin(\vartheta/2)$, λ and ϑ being the wavelength of the monochromatic X-ray beam and the angle between the incident and the scattered beam, respectively, t is a variable defined along the length of the line-shaped primary X-ray beam with its intensity distribution function $P(t)$ [20], $F(x)$ is the form factor of a sphere of radius r given by

$$F(x) \propto \frac{\sin(x) - x\cos(x)}{x^3} \quad , \tag{2}$$

where

$$x = r\sqrt{q^2 + t^2} \tag{3}$$

and $n(r)$, the size distribution function, is well-described by the Weibull equation

$$n(r) = A\left(\frac{r}{r^0}\right)^{b-1} \exp\left[-\left(\frac{r}{r^0}\right)^b\right] \quad . \tag{4}$$

In this equation, A is a constant, b is a parameter controlling the shape of the size distribution function

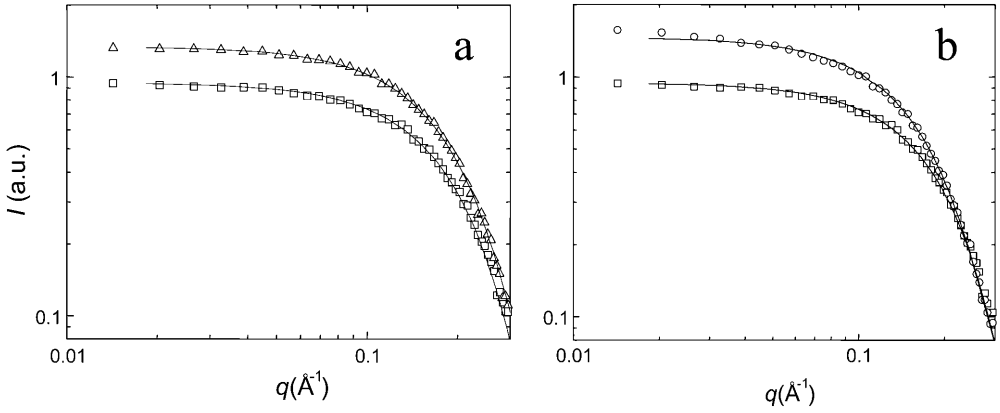

Fig. 2a, b Typical smeared scattering profiles and fitting curves of salt-containing resuspensions at $R_s = 0.13$ ($ZnSO_4$: △, Na_2S: ○) compared to that of AOT/*n*-heptane solution (□, in both plots)

and r^0 is a parameter related to the sphere mean radius, r_m, through the Γ function by

$$r_m = r^0 \Gamma\left(\frac{b+1}{b}\right) \quad . \tag{5}$$

Equation 4 is suitable for our purposes since it reduces to a simple exponential behaviour when the parameter b takes the value of 1, while with increasing b, it changes in a localised distribution around r_m. It is worth noting that SAXS originates from the contrast between different regions with different electron densities. Taking into account the peculiar structure of reversed micelles, r_m must be interpreted as the mean radius of the micellar core [21, 22].

Some fitting curves obtained by least-squares analysis through Eq. (1) are shown as continuous lines in Fig. 2. As can be seen, the curves reproduce within the experimental errors the scattering data. To save space, similar curve fittings for the other samples analysed in the present work are not reported. The derived parameters, r_m and b, are summarised in Table 1 and the size distribution functions of the core of AOT reversed micelles containing $ZnSO_4$ or Na_2S are shown in Fig. 3a and b, respectively. In this figure the size distribution function of the core of AOT reversed micelles at $R_s = 0$ is also reported for comparison.

An inspection of Table 1 reveals that r_m increases little with R_s for Na_2S-containing AOT micellar cores, whereas it is practically constant for $ZnSO_4$-containing ones. On the other hand, b displays a marked decrease, i.e. a marked increase in the particle size polydispersity in the presence of salts. These findings are consistent with a model of salt localised as very small nanoparticles in the micellar core of some AOT reversed micelles. In fact, the accumulation of salt as small nanoparticles within some reversed micelles involves an increase in their core size and surfactant aggregation number. As a consequence, the concentration of the remaining bare AOT reversed micelles decreases, leading to an increase in their polydispersity [23]. As a result of both effects, the overall polydispersity increases.

Table 1 Mean radius (r_m) and b values of the core of sodium bis(2-ethylhexyl)sulphosuccinate reversed micelles containing $ZnSO_4$ or Na_2S at various R_s

	R_s	r_m (Å)	b
$ZnSO_4$	0	10.4	18
	0.085	10.2	10
	0.13	10.4	10
	0.15	10.4	8.6
Na_2S	0.085	10.5	8.0
	0.13	11.2	12
	0.15	12.2	11

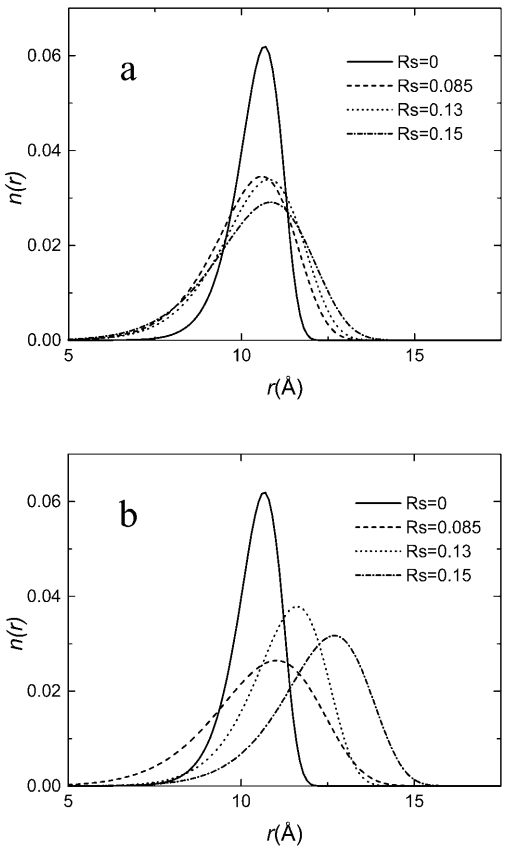

Fig. 3 Comparison of the size distribution functions derived from the analysis (see text) of the scattering data of salt-containing resuspensions at various R_s values (**a**: $ZnSO_4$, **b**: Na_2S) with that of the AOT/*n*-heptane solution ($R_s = 0$)

Let us now consider the results of the TEM investigation. It is of utmost importance to note that the preparation of the TEM samples necessarily requires the evaporation of resuspensions and the formation of salt/AOT composites. A typical TEM image is reported in Fig. 4 together with the statistical analysis of a Na_2S nanoparticles/AOT composite at $R_s = 0.13$. The presence of nearly spherical nanoparticles with radii ranging from 75 to 150 Å with a unimodal distribution and an average radius of 120 Å can be noted. Apart from rare clusters of nanoparticles, only isolated and randomly distributed nanoparticles can be observed. The comparison between the sizes found by TEM and SAXS suggests that solvent evaporation involves a drastic salt aggregation process and the formation of Na_2S nanoparticles bigger than those in solution. In contrast, as a consequence of the intermicellar material exchange process [24, 25], reversed micelles stabilise small Na_2S nanoparticles in solution.

A typical TEM image of a $ZnSO_4$/AOT composite at $R_s = 0.15$ is reported in Fig. 5, showing part of a big cluster of interacting $ZnSO_4$ nanoparticles. The statistical analysis of high magnification images, as that

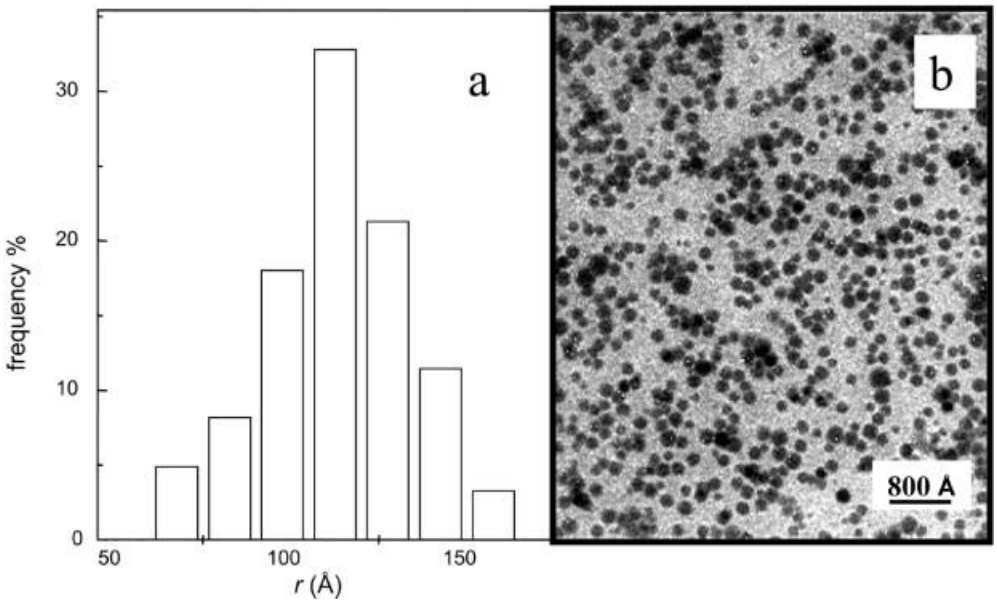

Fig. 4 **a** Statistical analysis and **b** typical micrograph of a Na_2S/AOT composite at $R_s = 0.13$

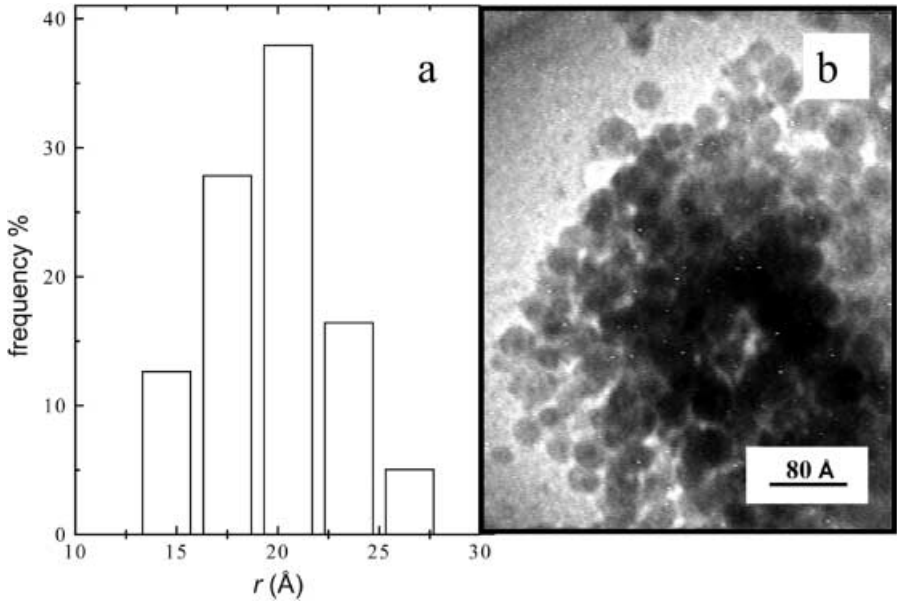

Fig. 5 **a** Statistical analysis and **b** typical micrograph of a $ZnSO_4$/AOT composite at $R_s = 0.15$

of Fig. 5b, reveals a unimodal size distribution with a mean nanoparticle radius of about 20 Å. It must be noted that also in the case of $ZnSO_4$/AOT composites, evaporation of organic solvent involves salt aggregation but, unlike Na_2S/AOT composites, this leads to the formation of interacting surfactant-coated nanoparticles. This finding would imply the existence of a relatively strong Zn–surfactant polar head interaction and, consequently, the formation of a layer of AOT molecules strongly adsorbed on the $ZnSO_4$ nanoparticle surface.

In order to investigate the feasibility of nanoparticle–nanoparticle reactions and also in view of a novel method for the synthesis of ZnS Q dots, we recorded the UV spectrum of the sample obtained by mixing equal amounts of two resuspensions at the same R_s value ($R_s = 0.13$) containing $ZnSO_4$ and Na_2S, respectively. It is shown in Fig. 6 together with the UV spectra of the resuspensions before mixing. It is evident that in the mix a new band centred at about 230 nm appears: this band can be easily attributed to the typical electronic absorption of ZnS Q dots [26]. From the position of the band maximum (λ_{max}) the ZnS nanoparticle diameter (d) can be calculated by the empirical relation [26, 27]

$$\lambda_{max} = 186.7 d^{0.13} \quad (6)$$

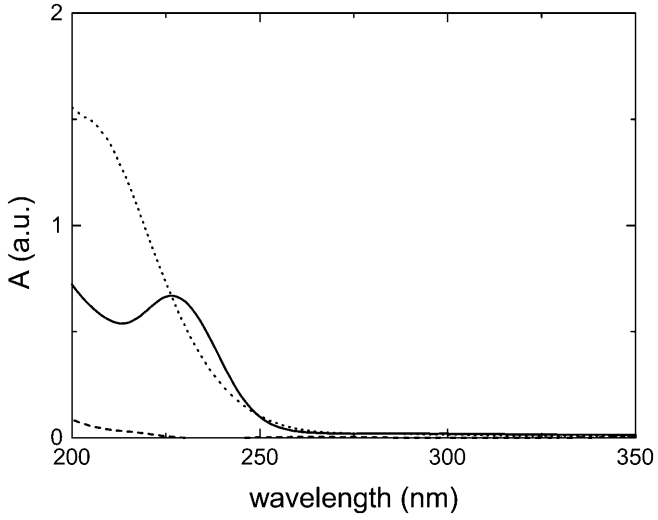

Fig. 6 UV spectra of salt-containing resuspensions (Na_2S: *dotted line*, $ZnSO_4$: *dashed line*, ZnS: *continuous line*)

The calculated ZnS nanoparticle diameter is very small (about 5 Å), suggesting that the present method could allow the synthesis of very small ZnS nanoparticles characterised by marked quantum size effects and enhanced photophysical properties. Furthermore, the concentration of ZnS in the AOT/*n*-heptane solution is very high, about 1 order of magnitude higher than that realised by means of w/o microemulsions [27].

Conclusions

This work proves that by evaporation of volatile components (water and organic solvent) of Na_2S- or $ZnSO_4$- containing w/o microemulsions, Na_2S/AOT and $ZnSO_4$/AOT composites containing nanoparticles of these salts can be obtained. Salt aggregation to form such nanoparticles has been interpreted to be possible, thanks to the water removal from salt-containing micellar aggregates in a sort of "confined crystallisation". It has been found that composites could be totally suspended in *n*-heptane, allowing the solubilisation of a relatively high amount of hydrophilic salt in a dry apolar medium. By SAXS it has been ascertained that salts are solubilised as small-sized nanoparticles.

TEM investigation of the salt/AOT composites provides nanoparticle radii in such systems: 13–27 Å for $ZnSO_4$ and 75–150 Å for Na_2S. In the case of $ZnSO_4$/AOT composites, the nanoparticles aggregate to form big nanoparticle clusters, while for Na_2S/AOT composites the TEM images show noninteracting nanoparticles.

Finally, the feasibility of the Na_2S–$ZnSO_4$ nanoparticle–nanoparticle reaction by simply mixing the salt-containing resuspensions, leading to the formation of small-sized ZnS nanoparticles, has been proved by UV spectrophotometry.

Acknowledgement Financial support from CNR and MURST 60% is gratefully acknowledged.

References

1. Rama Krishna MV, Friessner RA (1991) J Chem Phys 95:8309–8322
2. Tricot YM, Fendler JH (1986) J Phys Chem 90:3369–3374
3. Drexler KE (1992) Nanosystems. Wiley, New York
4. Esquena J, Tadros TF, Kostarelos K, Solans C (1997) Langmuir 13:6400–6406
5. Lin XM, Sorensen CM (1998) Langmuir 14:7140–7146
6. Li Y, Park CW (1999) Langmuir 15:952–956
7. Fendler JH (1987) Chem Rev 87:877–899
8. Turco Liveri V (1999) Curr Top Colloid Interface Sci 3:65–74
9. Towey TF, Khan-Lodhi A, Robinson BH (1990) J Chem Soc Faraday Trans 86:3757–3762
10. Eastoe J, Warne B (1996) Curr Opin Colloid Interface Sci 1:800–805
11. Cizeron J, Pileni MP (1995) J Phys Chem 99:17410–17416
12. Arcoleo V, Cavallaro G, La Manna G, Turco Liveri V (1995) Thermochim Acta 254:111–119
13. Aliotta F, Arcoleo V, Buccoleri S, La Manna G, Turco Liveri V (1995) Thermochim Acta 256:15–23
14. Arcoleo V, Turco Liveri V (1996) Chem Phys Lett 258:223–227
15. D'Aprano A, D'Arrigo G, Paparelli A, Goffredi M, Turco Liveri V (1993) J Phys Chem 97:3614–3618
16. Marcianò V, Minore A, Turco Liveri V (2000) Colloid Polym Sci 278:250–252
17. Sooklal K, Cullum BS, Angel SM, Murphy CJ (1996) J Phys Chem 100:4551–4555
18. Reber JF, Meir K (1984) J Phys Chem 88:5903–5913
19. Arcoleo V, Goffredi M, Turco Liveri V (1998) J Colloid Interface Sci 198:216–223
20. Ruland W (1974) J Appl Crystallogr 7:383–386
21. North AN, Dore JC, McDonald JA, Robinson BH, Heenan RK, Howe AM (1986) Colloids Surf 19:21–29
22. Mackeben S, Müller-Goymann CC (2000) Int J Pharm 196:207–210
23. Hirai M, Kawai-Hirai R, Yabuki S, Takizawa T, Hirai T, Kobayashi K, Amemiya Y, Oya M (1995) J Phys Chem 99:6652–6660
24. Fletcher PDI, Robinson BM (1981) Ber Bunsen-Ges Phys Chem 85:863–867
25. Clarke J, Nicholson J, Regan K (1985) J Chem Soc Faraday Trans 89:1173–1182
26. Nakaoka Y, Nosaka Y (1997) Langmuir 13:708–713
27. Calandra P, Goffredi M, Turco Liveri V (1999) Colloids Surf A 160:9–13